RSC Advances

ROYAL SOCIETY OF CHEMISTRY

www.rsc.org/advances

RSC Advances

ARTICLE

Seedless synthesis of gold nanorods using dopamine as a reducing agent

Received 25th September 2015,
Accepted 00th January 20xx

DOI: 10.1039/x0xx00000x

www.rsc.org/

Anton Liopo,[a,b] Shaowei Wang,[a,c] Paul J. Derry,[a] Alexander A. Oraevsky,[b] and Eugene R. Zubarev[a*]

A novel protocol for the seedless synthesis of gold nanorods (AuNRs) using dopamine as a reductant has been developed. We report that the concentration of CTAB can be reduced to 22 mM and that the AuNRs longitudinal surface plasmon resonance (LSPR) can be tuned from 700 to 1050 nm. The size of AuNRs can also be tuned from 7 x 30 nm to 20 x 100 nm. The amphiphilicity and the cationic structure of the protonated dopamine enable it to interact favorably with the CTAB bilayer and lead to a high-yield synthesis of AuNRs (80-95%). LSPR peaks, size, and aspect ratio of the synthesized AuNRs can be tuned by adjusting the concentration and ratio of silver ions, CTAB, and dopamine. In addition, this reaction is much faster than previously reported methods requiring only 30 minutes to complete.

Introduction

Gold nanorods (AuNRs) have attracted significant interest as a platform for nanobiotechnology. The unique optical properties of AuNRs arise from the interaction of photons with surface electrons which give rise to a surface plasmon resonance (SPR).[1] The overall size and morphology of a gold nanorod modulate the SPR and result in a strong optical absorption and scattering at visible and near-infrared wavelengths.[2–4] These properties have been utilized in cancer therapy research with applications in imaging[5–8] and photothermal therapeutics.[7,9,10] In addition, AuNRs have been used to enhance light absorption in photovoltaic devices and as surface enhanced Raman spectroscopy (SERS) substrates.[11,12]

Most AuNR syntheses fall into one of four categories: electrochemical,[13] photochemical,[14] seed-mediated,[15] and templated methods.[16] The most reliable method is the seed-mediated synthesis introduced by El-Sayed et al.[15] and Murphy et al.[17] in which cetyltrimethylammonium bromide (CTAB) and silver nitrate control the growth of anisotropic nanocrystals. El-Sayed and co-workers described the synthesis of AuNRs with LSPR up to 1000 nm through the use of a mixed surfactant system CTAB/BDAC (benzyldimethylhexadecyl-ammonium chloride).[15] Other factors such as temperature,[18] pH,[19] the type of surfactant,[20–22] reagents concentration,[17] aromatic additives,[22,23] and the seed quality[24] are also known to influence the growth and purity of AuNRs.

In situ seed formation, or "seedless" growth was initially reported by Jana et al. in 2001.[25] In a seedless synthesis, AuNRs are synthesized by directly adding $NaBH_4$ into a growth solution containing Au(I) ions, silver nitrate, CTAB, and ascorbic acid.[26] However, this method produces highly polydisperse AuNRs with a large amount of spherical particles. Recently, a variation of the seedless protocol has been developed for smaller nanorods.[27]

It is well-known that phenolic and polyphenolic compounds can function as mild reducing agents. Although their reduction potentials are typically lower than ascorbic acid, they are able to reduce Au(III) to Au(I) at room temperature. Vigderman et al. reported that hydroquinone could be successfully used as a drop-in replacement for ascorbic acid in the seed-mediated synthesis of AuNRs.[28] Similarly, Zhang and co-workers reported that 1,2,3-trihydroxybenzene and 1,2,4-trihydroxybenzene are also suitable for that purpose.[29] In addition, dopamine (DA) was found to be an effective reductant in the synthesis of spherical gold,[30] silver,[31,32] zinc oxide,[33] and iron oxide nanoparticles.[34] Besides the reducing ability of dopamine, its oxidation byproduct, polydopamine, can be used as a nanoparticle stabilizer.[30] Recently, Su et al. reported the first synthesis of AuNRs using dopamine in a seed mediated protocol and demonstrated its high efficiency.[35]

However, the use of DA in the *seedless synthesis of AuNRs* has not been reported to date. Here we describe a tunable and facile method for the controlled seedless synthesis of AuNRs using dopamine as a reductant at CTAB concentrations well below previously reported values and at room temperature.

Experimental

Materials

CTAB, silver nitrate, hydrogen tetrachloroaurate trihydrate, sodium borohydride, hydrochloric acid, nitric acid, gold standard solutions, and dopamine hydrochloride were purchased from Sigma-Aldrich. All solutions were prepared fresh prior to use except for the $HAuCl_4$ and CTAB solutions. AuNRs synthesized with hydroquinone were used as a control throughout these experiments. Detailed procedures can be found in Supporting Information.

[a] Department of Chemistry, Rice University, Houston, Texas 77005, USA
[b] TomoWave Laboratories Inc. Houston, Texas 77081, USA
[c] Current address: Center for Optical and Electromagnetic Research, Zhejiang University, Hangzhou 310058, China
† Corresponding author: zubarev@rice.edu
Electronic Supplementary Information (ESI) available: See DOI: 10.1039/x0xx00000x

Seedless Synthesis of Gold Nanorods with Dopamine

In a typical synthesis, 5 mL of CTAB (50 mM) was placed in a 25 mL glass vial followed by 500 µL of dopamine aqueous solution (500 mM) and the mixture was allowed to stir for 10 min. Next, 5 mL of $HAuCl_4$ aqueous solution (1 mM) was added and stirred for another 10 min. At that point, 100 µL of $AgNO_3$ solution (200 mM) was added followed by the addition of 500 µL of dopamine (500 mM). Finally, the stirring rate was increased to 1200 RPM and 10 µL of $NaBH_4$ aqueous solution (10 mM, ice cold) was added in a single injection to the vial. The stirring was stopped and the reaction mixture was kept at 25 °C for several hours. The as-synthesized AuNRs were purified by centrifugation at 10,000 RCF and redispersed into Milli-Q water.

Dynamics of Dopamine Synthesis of AuNRs

AuNRs growth was monitored using a Cary 5000 UV-vis-NIR spectrophotometer equipped with a temperature-controlled cuvette holder set to 28 °C. AuNRs growth solution was prepared as described above and an aliquot was placed in the spectrophotometer immediately after the addition of $NaBH_4$ to initiate the growth. Spectra were collected between 400 and 1400 nm every 5 minutes for the first 25 minutes, and every 25 minutes for the following 150 minutes.

Gold Nanorod Characterization

Inductively Coupled Plasma – Optical Emission Spectrometry (ICP-OES) Analysis. A 11 mL batch of AuNRs solution prepared from $5.0x10^{-6}$ mol $HAuCl_4$ was isolated after 2.5 h of AuNRs growth and centrifuged at 20,000 RCF followed by the addition of 10 mL acetone. The precipitated AuNRs were rinsed carefully with Milli-Q H_2O to remove residual CTAB and acetone and then dried under a nitrogen flow. The resulting AuNRs were digested with *aqua regia* (3:1 HNO_3:HCl) and diluted to 10 mL with 1% HCl as a stock solution. ICP-OES analysis was performed on a 10:1 dilution of the stock solution. The calculated yield of gold ions to metallic gold conversion was 88%. Transmission electron microscopy imaging was performed on a JEOL-1230 (JEOL) instrument operating at 80 kV. High resolution transmission electron micrographs were obtained on a JEOL-2100F (JEOL) field effect gun transmission electron microscope operating at 200 kV. UV-vis spectra were obtained on a Cary 5000 (Varian) UV-vis-NIR spectrophotometer. All solutions were measured using polymethylmethacrylate cuvettes (1 x 4 cm). Nanorods size distribution calculations and TEM analysis was performed using ImageJ (National Institutes of Health).

Results and Discussion

Dopamine (DA) is a redox-active catecholamine neurotransmitter involved in many physiological processes.[36] DA can undergo enzymatic oxidation through the actions of transition metals, as well as spontaneous auto-oxidation with atmospheric oxygen.[37] DA oxidation occurs via a one- or two-electron reaction and results in the formation of a semi-quinone radical and subsequently dopamine-*o*-quinone (DQ), a precursor to melanin as confirmed by EPR and NMR.[38,39]

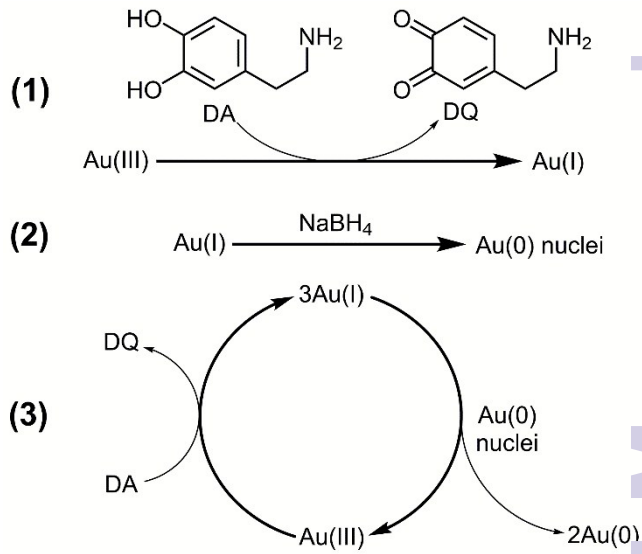

Scheme 1. Reaction scheme of AuNRs preparation with dopamine (DA) as a reductant.

Scheme 1 shows the reduction of Au(III) to Au(I) by the oxidation of DA (stage 1) and further reduction of Au(I) to Au(0) by sodium borohydride to produce initial gold nuclei (stage 2). The subsequent deposition of gold onto the nuclei and the ensuing growth of AuNRs is due to disproportionation of Au(I) ions, which is known to be catalyzed by metallic gold surface.[40] The DA molecules play the role of a scavenger for Au(III) ions that are generated in the course of this disproportionation reaction and quickly convert them to Au(I), thus completing the catalytic cycle (stage 3). This is essentially the same role played by ascorbic acid in a conventional seed-mediated synthesis.[15,17] Both ascorbic acid and DA are not strong enough reducing agents to convert Au(I) directly to Au(0), but they are necessary sources of electrons that allow the disproportionation reaction to proceed and continuously convert nearly all Au(I) ions to metallic gold. However, Su and co-workers[35] have recently reported that the seed-mediated synthesis of AuNRs requires a large excess of DA. This observation was also consistent with the results of Vigderman et al.[28] when using hydroquinone as a scavenger of Au(III) ions.

It is important to differentiate the role of $NaBH_4$ from that of DA in our synthesis. The molar ratio of $NaBH_4$ versus Au(I) is typically 1:50, which means that no more than 8% of Au(I) ions can be converted to metallic gold by $NaBH_4$ even if all four hydride ions are used for reduction (stage 2 in Scheme 1). Thus, $NaBH_4$ only generates the initial nuclei that are necessary to catalyze the disproportionation of Au(I) ions (Stage 3). The subsequent growth of AuNRs is solely due to the deposition of Au(0) generated from the disproportionation reaction. To corroborate this idea we performed ICP-OES analysis and determined that 88 % of gold ions have been converted to metallic gold after 2.5 h. This implies that the overall yield of conversion is considerably higher than that in classical seed-mediated procedures.[15,17]

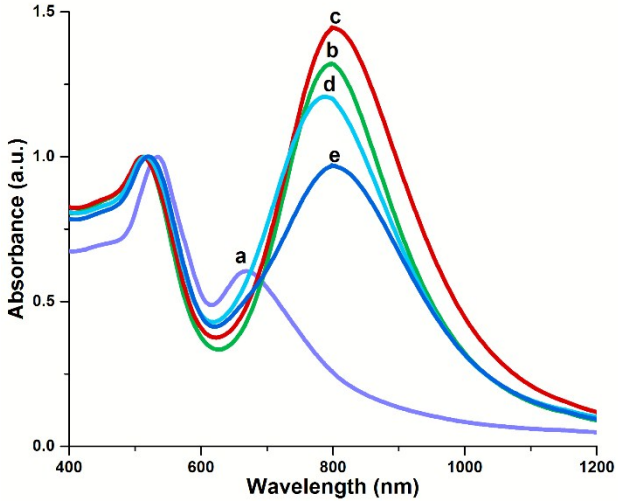

Figure 1. UV-Vis spectra of AuNRs synthesized with different DA concentrations: [DA] = 13.5, 27, 45, 67.5, and 90 mM: a, b, c, d, e respectively. Final concentrations: [CTAB] = 22 mM, [$HAuCl_4$] = 0.45 mM, [$AgNO_3$] = 0.91 mM, and [$NaBH_4$] = 0.018 mM.

Aside from its ability to act as a reducing agent, DA can also stabilize the surface of growing AuNRs due to its amphiphilic character. This may be beneficial for the synthesis of anisotropic nanostructures.[41] The FTIR spectra of seed-mediated gold nanorods synthesized with DA were reported by Su and suggested the presence of DA at the surface of AuNRs.[35] These authors have also shown that LSPR can be tuned at low CTAB concentration. Therefore, the DA may play a dual role in the seedless preparation of AuNRs: reducing Au(III) to Au(I) and aiding the growth of the AuNRs by mediating the binding between CTAB and the growing AuNRs. This binding may enable a significant reduction in the amount of CTAB required for the successful synthesis of nanorods, which is known to be the most expensive reagent in the conventional El Sayed –Murphy synthesis.[15,17]

It is well known that additives such as salicylates and other aromatic species play an important role in the monodispersity, morphology, and shape-yield of the resulting AuNRs.[22] Our experiments show that DA does not act solely as a reductant, but also has a stabilizing effect on the synthesized AuNRs. Fig. 1 shows the UV-vis spectra of AuNRs synthesized with DA (13.5 to 90 mM.) When 13.5 mM (Fig. 1a) of dopamine was used, the yield was poor and the LSPR peak was around 670 nm. As the concentration was increased to 27 mM (Fig. 1b) and then to 45 mM (Fig. 1c), the LSPR showed a red shift to 795 and 805 nm, respectively. When the amount of dopamine increased beyond 67.5 mM (Figs. 1d, 1e) the LSPR peak slightly blue-shifted, but there was a considerable reduction in its intensity. These results suggest that exceeding a certain concentration of DA may not reduce the aspect ratio of AuNRs, but can decrease their yield in comparison to spherical impurities.

Along with the overall concentration of DA, we investigated the effect of its addition in several increments and in a different order during the reaction. We found that the addition of DA in the following order provided the best results: CTAB (1) + DA (2, ½ volume) + $HAuCl_4$ (3), + $AgNO_3$ (4), + DA (5, ½ volume) and $NaBH_4$ (6). We tested three different DA addition orders: a) ½ DA + ½ DA; b) H_2O+DA; c) DA+H_2O (Fig. S1). We obtained the best results by performing the two-part

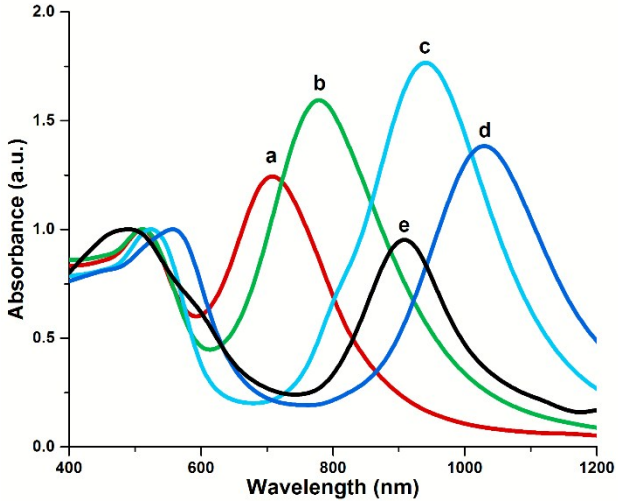

Figure 2. The effect of CTAB concentration on AuNR UV-Vis spectra: [CTAB] = 9, 22, [illegible] 90, and 180 mM (lines a, b, c, d, and e respectively). Other parameters: [DA] = 45 mM [$HAuCl_4$] = 0.45 mM, [$AgNO_3$] = 1.82 mM, and [$NaBH_4$] = 0.018 mM.

addition of DA before and after the addition of silver nitrate. Additionally, we examined the influence of temperature and the concentration of gold ions on LSPR peak in order to identify the best set of conditions (Fig. S2, S3).

AuNRs could be grown in solutions with CTAB concentrations well below 0.1 M because both DA and resulting DQ can stabilize the growing nanorods. Our procedure allows for the synthesis of AuNRs from CTAB solutions with concentrations as low as 9 mM. We examined a CTAB concentration range between 9 and 180 mM (Fig. 2) and observed a gradual LSPR red-shift from 730 nm for (9 mM CTAB) to 1040 nm (90 mM CTAB). At 180 mM, however, the LSPR blue-shifted to 915 nm accompanied by an overall loss in the yield and quality of AuNRs. The general trend is that the aspect ratio of AuNRs initially increases directly with the concentration of CTAB, but there is a threshold concentration that when surpassed leads to a reduction in the wavelength and intensity of the LSPR peak (Fig. S7C). This may be related to high solution viscosity at CTAB concentration above 100 mM and the formation of insoluble silver bromide.

Ye et al.[22] have recently reported that aromatic additives such as salicylates can intercalate with CTAB bilayers and modulate the geometry of AuNRs. In addition, they demonstrated that the concentration of CTAB could be reduced to as low as 50 mM without compromising the quality of nanorods. One can envision that DA, and especially the resulting DQ, are also able to incorporate into CTAB bilayers given their amphiphilic structure and the positively charged polar head (protonated amino group).

The pH of the growth solution was previously shown to have a direct impact on the size and quality of AuNRs prepared with sodium oleate as a reducing agent.[42] We anticipated that such a phenomenon could also occur with dopamine. To test this hypothesis, we included a small amount of HCl and found

that after 24 h of growth with variable concentrations of HCl (0 to 4.0 µM), the decrease in pH value had a detrimental effect on the quality and shape-yield of AuNRs. Figure S4 shows that in the growth solutions with 0.5 µM HCl the LSPR shifts from 820 nm to 835 nm. However, at higher concentrations (1-4 µM) the peak blue-shifts to lower wavelengths and the longitudinal-to-transverse plasmon ratio decrease significantly.

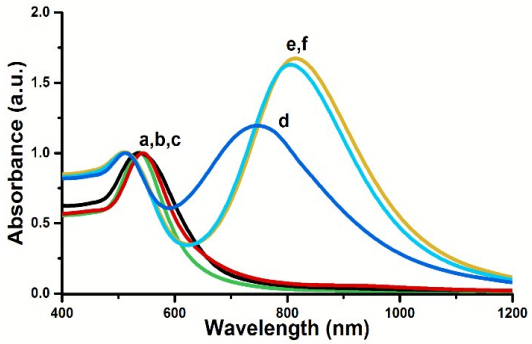

Figure 3. AuNR UV-Vis spectra at different concentrations of silver nitrate: [$AgNO_3$] = 0.9, 4.5, 9.1, 22, 45, and 91 µM (lines **a**,**b**,**c**,**d**,**e**, and **f**, respectively). Other parameters: [CTAB] = 22 mM, [DA] = 45 mM, [$HAuCl_4$] =0.45 mM, and [$NaBH_4$] = 0.018 mM.

The reduction in yield and blue-shift of the LSPR suggest that under strong acidic conditions the oxidation of DA is much slower, which is consistent with kinetic studies of hydroquinones oxidation as a function of pH.[39]

We also investigated the relationship between the LSPR and the final concentration of $NaBH_4$. We examined a concentration range of $NaBH_4$ from 0 to 36 µM with results presented in Fig. S5. The concentration of $NaBH_4$ that gives the highest LSPR wavelength was found to be 5 µM, and further increments resulted in a blue-shift of the peak. Interestingly, Ali and coworkers[27] performed a similar analysis of sodium borohydride concentration and observed a red shift of LSPR peak when the pH was in the range between 1 and 2 and ascorbic acid was used as a scavenger of Au(III) ions. Our growth solution had a higher pH (3-4) and required a $NaBH_4$ concentration of 10-20 µM for reproducible results. With these findings we can conclude that for seedless syntheses the type of reducing agent and the molar ratio between CTAB, $AgNO_3$ and $NaBH_4$ play an important role in determining the overall yield and morphology of AuNRs.

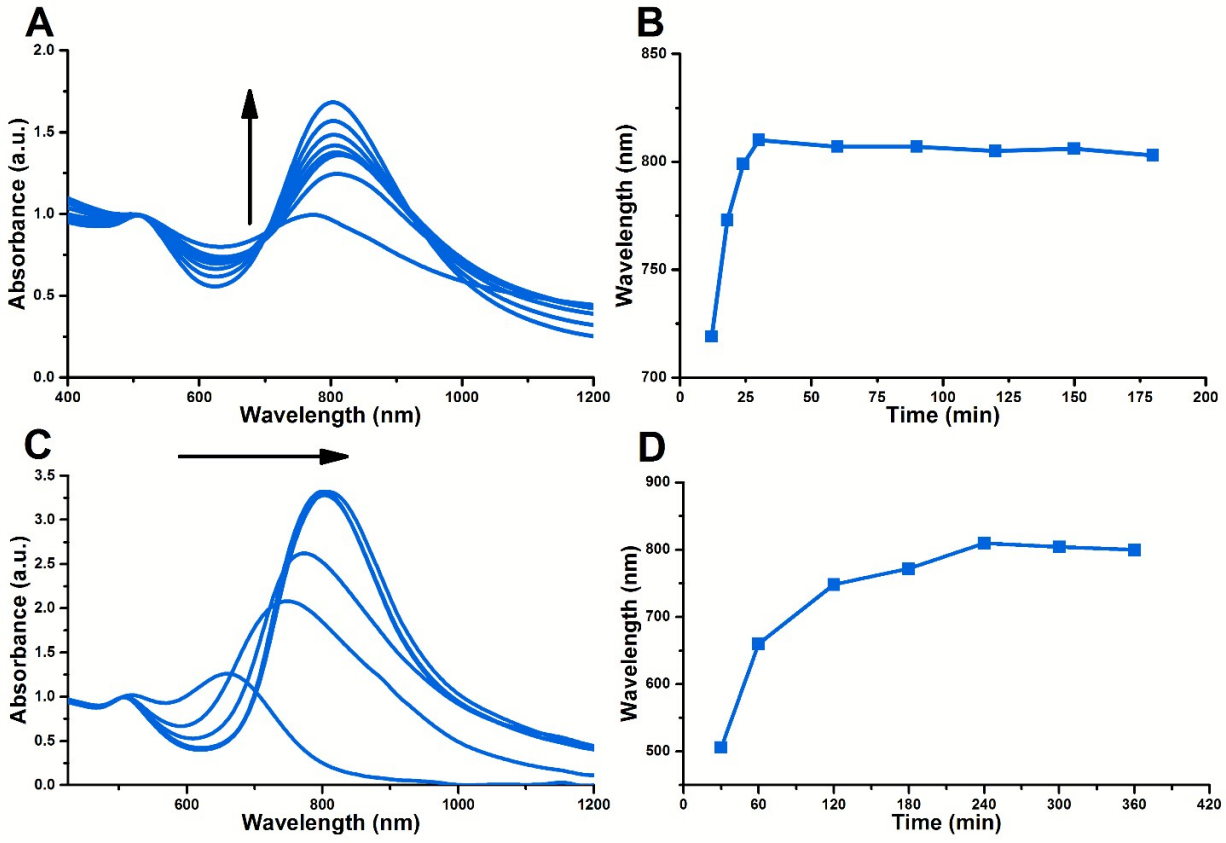

Figure 4. Evolution of the UV–vis spectra during the synthesis: AuNRs prepared by reduction with DA (A, B) and hydroquinone (C, D) using a similar seedless protocol (see SI for details).

It is well-known that changes in silver nitrate concentration can influence the aspect ratio of AuNRs. We tested the effect of varying the Ag^+ concentration in 22 mM and 90 mM CTAB growth solutions by adding increasing amounts of 100 mM $AgNO_3$ solution (Fig. 3, Fig. S6). We observed a single UV-vis peak at 525 nm when $AgNO_3$ concentration was in the range from 0.9 µM to 9 µM, which suggested the formation of only spherical nanoparticles. However, at the concentrations from 9

to 90 μM the wavelength of LSPR peak was tunable, but only to a small extent. We believe that the fairly narrow range of achievable LSRPs in 22 mM CTAB is mainly due to the low solubility of Ag^+ in halide-containing solutions. This is very

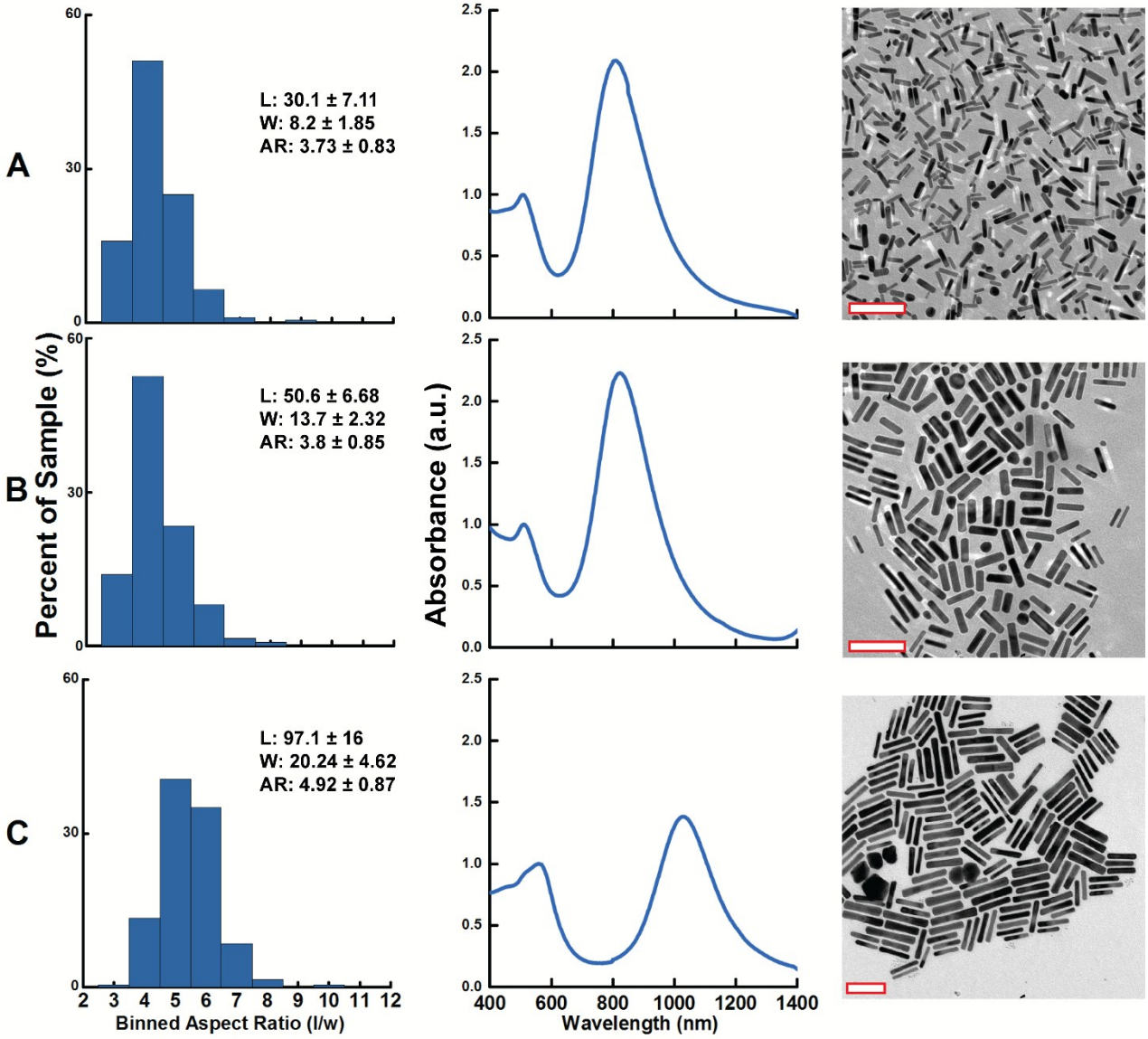

Figure 5. Size distribution, UV–Vis spectra and TEM images of AuNRs synthesized by reduction with dopamine under different conditions (see Figs. S7A, S7B and S7C, respectively). Length (L) and width (W) are in nm. Scale bars in TEM images are 100 nm.

similar to the preparation of AuNRs when ascorbic acid is used.[15] Work by Xu et al. showed that the seedless synthesis of AuNRs is also similarly affected by the high concentration of Ag^+ and CTAB.[43]

The evolution of the UV-Vis spectra of AuNRs during their growth is illustrated in Fig. 4. The spectra are different for each protocol, but both have similar trends with red-shifting and stabilization. However, for dopamine-synthesized AuNRs (Fig. 4a, b) the process is much faster and the LSPR quickly stabilizes after 25-30 min from the start of the synthesis, whereas for hydroquinone-synthesized AuNRs (Fig. 4c, d) it stabilizes only after 240 min. This is an important advantage of the reported synthesis, which provides an opportunity to produce AuNRs in a much quicker fashion than conventiona protocols.

Table 1. Calculated volumes and shape-yield of samples 5A, 5B, 5C.

Sample	Volume (nm^3)	Shape Yield (%)
5A	1600	80
5B	7450	90
5C	31100	94

Size distribution, absorbance spectra, and TEM images a presented for gold nanorods synthesized by reduction with dopamine in Fig. 5. Samples 5A and 5B have similar aspect ratios: 3.7 ± 0.8 and 3.8 ± 0.9; but with different dimensions of 30.1 × 8.2 and 50.6 × 13.7 nm, respectively. Sample 5A w s

prepared with a low concentration of CTAB (22 mM), 27 mM dopamine, and 0.91 mM silver nitrate. The average volume of AuNRs in sample 5A is 1600 nm^3, whereas the shape-yield is close to 80%. Sample 5B was prepared with the same concentrations of CTAB (25 mM) and dopamine (27 mM), but the $AgNO_3$ concentration was doubled (1.82 mM). This change led to an increase in the average volume and shape-yield of AuNRs to 7450 nm^3 and 90%, respectively. In contrast, sample 5C was prepared with high concentration of CTAB (100 mM) and dopamine 45 mM, but the same silver nitrate concentration of 1.82 mM. The average volume of AuNRs in this case increases to 31100 nm^3, which is nearly 20 times higher, but the shape-yield still remains very high (~ 95%). The size distribution of AuNRs is fairly narrow (Fig. 5) indicating a reliable morphological control for each synthesis (details of AuNR preparations and additional TEM images are available in Fig. S7). Our synthesis demonstrates that yields in excess of 90% are possible for a seedless protocol, which compares favorably to previously reported methods.[29] These examples illustrate the robust and flexible nature of dopamine as a reducing agent for the preparation of AuNRs with tunable sizes and aspect ratios.

Conclusions

In summary, we have developed an efficient seedless method for the preparation of gold nanorods using dopamine as a reducing agent. This very fast single-step method has a high capacity for the controlled synthesis of anisotropic nanocrystals. Gold nanorods were successfully prepared with LSPRs ranging between 700 and 1050 nm. The synthetic parameters for AuNRs with different lengths, widths, and aspect ratio were successfully identified through a systematic study. LSPR peaks and the overall morphology of the synthesized AuNRs could be tuned by adjusting the concentration and the ratio of silver ions, CTAB, and dopamine. This method may bring additional insights and a better understanding of the seedless synthesis of other nanomaterials.

Acknowledgements

The authors are thankful to the NSF (DMR-1105878) and John Dunn Foundation for the financial support provided for this research.

Notes and references

1 M. A. El-Sayed, *Acc. Chem. Res.*, 2001, **34**, 257–264.
2 A. Oraevsky, in *Photoacoustic Imaging and Spectroscopy*, 2009, pp. 373–386.
3 A. M. Alkilany, L. B. Thompson, S. P. Boulos, P. N. Sisco and C. J. Murphy, *Adv. Drug Deliv. Rev.*, 2012, **64**, 190–199.
4 H. Chen, L. Shao, Q. Li and J. Wang, *Chem. Soc. Rev.*, 2013, **42**, 2679–2724.
5 C. Loo, A. Lowery, N. J. Halas, J. West and R. Drezek, *Nano Lett.*, 2005, **6**, 709–711.
6 N. J. Durr, T. Larson, D. K. Smith, B. A. Korgel, K. Sokolov and A. Ben-Yakar, *Nano Lett.*, 2007, **7**, 941–945.
7 X. Huang, I. H. El-Sayed, W. Qian and M. A. El-Sayed, *J. Am. Chem. Soc.*, 2006, **128**, 2115–2120.
8 A. Liopo and A. Oraevsky, in *Nanotechnology for Biomedical Imaging and Diagnostics: From Nanoparticle Design to Clinical Application*, ed. M. Berezin, John Wiley and Sons, 2015, pp. 111–149.
9 V. P. Zharov, K. E. Mercer, E. N. Galitovskaya and M. S. Smeltzer, *Biophys. J.*, 2006, **90**, 619–627.
10 L. Vigderman, P. Manna and E. R. Zubarev, *Angew. Chem. Int. Ed.*, 2012, **51**, 636–641.
11 H. A. Atwater and A. Polman, *Nat. Mater.*, 2010, **9**, 865.
12 S. J. Tan, M. J. Campolongo, D. Luo and W. Cheng, *Nat. Nanotechnol.*, 2011, **6**, 268–276.
13 Yu, S.-S. Chang, C.-L. Lee and C. R. C. Wang, *J. Phys. Chem. B*, 1997, **101**, 6661–6664.
14 F. Kim, J. H. Song and P. Yang, *J. Am. Chem. Soc.*, 2002, **124**, 14316–14317.
15 B. Nikoobakht and M. A. El-Sayed, *Chem. Mater.*, 2003, **15**, 1957–1962.
16 C. Gao, Q. Zhang, Z. Lu and Y. Yin, *J. Am. Chem. Soc.*, 2011, **133**, 19706–19709.
17 T. K. Sau and C. J. Murphy, *Langmuir*, 2004, **20**, 6414–6420.
18 L. Gou and C. J. Murphy, *Chem. Mater.*, 2005, **17**, 3668–3672.
19 B. D. Busbee, S. O. Obare and C. J. Murphy, *Adv. Mater.*, 2003, **15**, 414–416.
20 A. Guerrero-Martínez, J. Pérez-Juste, E. Carbó-Argibay, G. Tardajos and L. M. Liz-Marzán, *Angew. Chemie Int. Ed.*, 2009, **48**, 9484–9488.
21 R. C. Wadams, L. Fabris, R. A. Vaia and K. Park, *Chem. Mater.*, 2013, **25**, 4772–4780.
22 X. Ye, L. Jin, H. Caglayan, J. Chen, G. Xing, C. Zheng, V. Doan-Nguyen, Y. Kang, N. Engheta, C. R. Kagan and C. B. Murray, *ACS Nano*, 2012, **6**, 2804–2817.
23 J. S. DuChene, W. Niu, J. M. Abendroth, Q. Sun, W. Zhao, F. Huo and W. D. Wei, *Chem. Mater.*, 2013, **25**, 1392–1399.
24 X. C. Jiang and M. P. Pileni, *Colloids Surfaces A Physicochem. Eng. Asp.*, 2007, **295**, 228–232.
25 N. R. Jana, L. Gearheart and C. J. Murphy, *J. Phys. Chem. B*, 2001, **105**, 4065–4067.
26 N. R. Jana, *Small*, 2005, **1**, 875–882.
27 M. R. K. Ali, B. Snyder and M. A. El-Sayed, *Langmuir*, 2012, **28**, 9807–9815.
28 L. Vigderman and E. R. Zubarev, *Chem. Mater.*, 2013, **25**, 1450–1457.
29 L. Zhang, K. Xia, Z. Lu, G. Li, J. Chen, Y. Deng, S. Li, F. Zhou and N. He, *Chem. Mater.*, 2014, **26**, 1794–1798.
30 Y. Lee and T. G. Park, *Langmuir*, 2011, **27**, 2965–2971.
31 Y. Liao, Y. Wang, X. Feng, W. Wang, F. Xu and L. Zhang, *Mater. Chem. Phys.*, 2010, **121**, 534–540.
32 Y. Ma, H. Niu, X. Zhang and Y. Cai, *Analyst*, 2011, **136**, 4192.
33 W. Huang, P. Jiang, C. Wei, D. Zhuang and J. Shi, *J. Mater. Res.*, 2008, **23**, 1946–1952.
34 M. D. Shultz, J. U. Reveles, S. N. Khanna and E. E. Carpenter, *J. Am. Chem. Soc.*, 2007, **129**, 2482–2487.
35 G. Su, C. Yang and J.-J. Zhu, *Langmuir*, 2015, **31**, 817–823.
36 S. D. Iversen and L. L. Iversen, *Trends Neurosci.*, 2007, **30**, 188–193.
37 M. Akagawa, Y. Ishii, T. Ishii, T. Shibata, M. Yotsu-Yamashita, K. Suyama and K. Uchida, *Biochemistry*, 2006, **45**, 15120–15128.
38 A. H. Stokes, T. G. Hastings and K. E. Vrana, *J. Neurosci. Res.*, 1999, **55**, 659–665.
39 A. J. Kettle and C. C. Winterbourn, *J. Biol. Chem.*, 1992, **267**, 8319-8324.
40 C. H. Gammons, Y. Yu and a. E. Williams-Jones, *Geochim. Cosmochim. Acta*, 1997, **61**, 1971–1983.

41 Y. Xu, Y. Zhao, L. Chen, X. Wang, J. Sun, H. Wu, F. Bao, J. Fan and Q. Zhang, *Nanoscale*, 2015, **7**, 6790–6797.
42 X. Ye, C. Zheng, J. Chen, Y. Gao and C. B. Murray, *Nano Lett.*, 2013, **13**, 765–771.
43 X. Xu, Y. Zhao, X. Xue, S. Huo, F. Chen, G. Zou and X.-J. Liang, *J. Mater. Chem. A*, 2014, **2**, 3528.

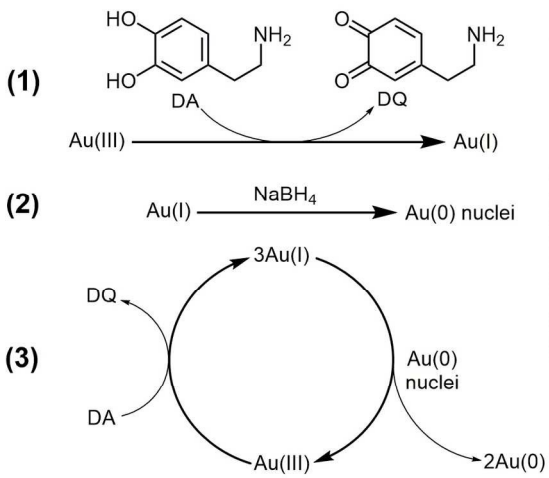

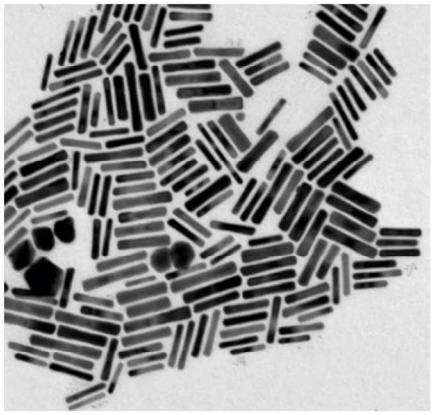

The first example of seedless synthesis of gold nanorods using dopamine as e reducing agent is described in this work.